

UDC 548.73:541.49:546.48

THREE METAL-ORGANIC POLYMERS ASSEMBLED FROM Cd(II)-FLUCONAZOLE: SYNTHESES, CRYSTAL STRUCTURES, AND CHARACTERIZATION

C.-J. Lin¹, L.-X. Zhou², Q.-J. Niu¹, Y.-Q. Zheng¹, H.-L. Zhu¹, B.-B. Zhang¹

¹*Crystal Engineering Lab, Research Center for Solid State Chemistry & Application, Ningbo University, Ningbo, P. R. China*

E-mail: yqzhengmc@163.com

²*Zhejiang Zhong Hao Applied Engineering Technique Institute Co., Ltd., Hangzhou, P. R. China*

Received December, 21, 2014

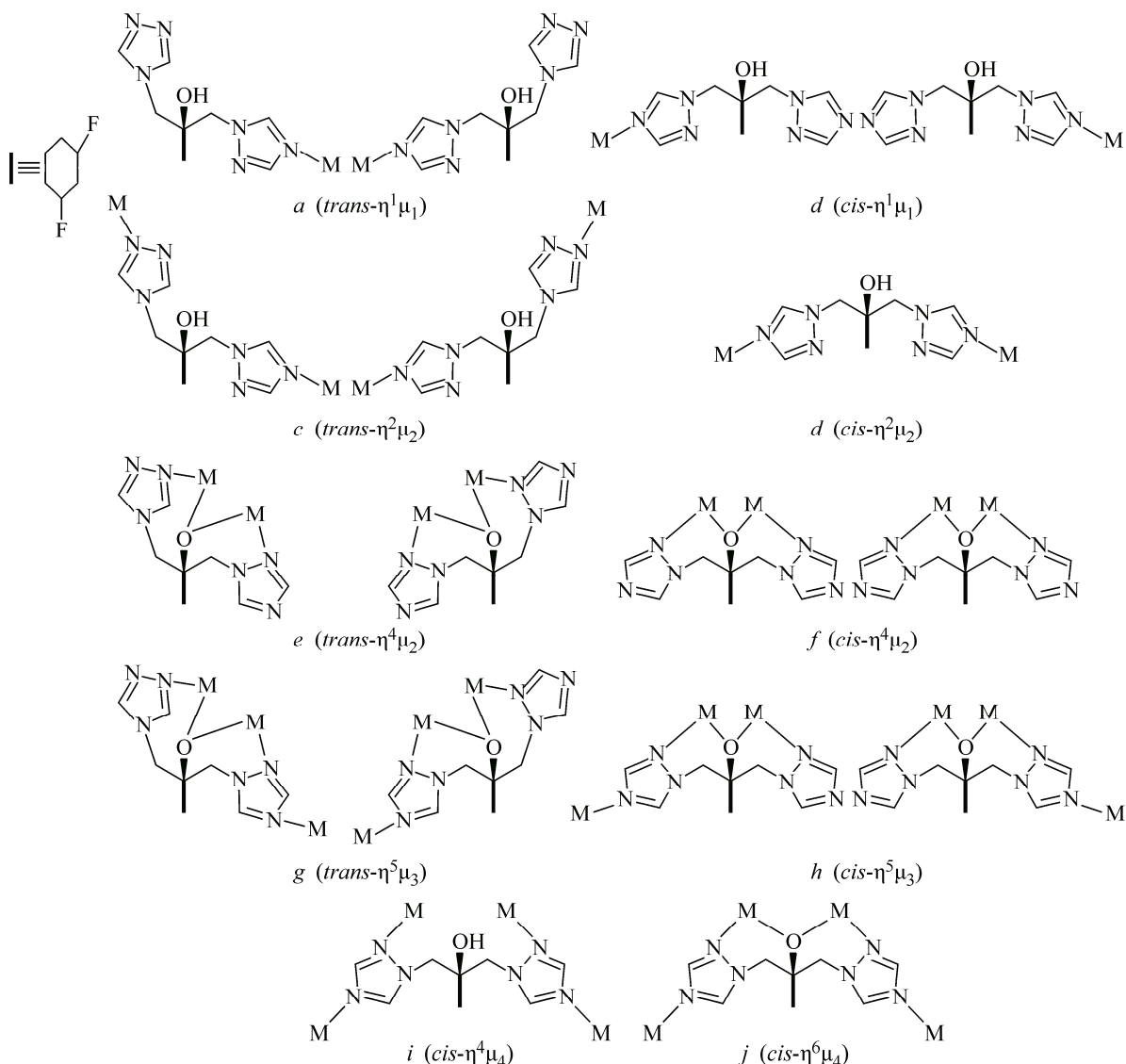
Three new complexes $[\text{Cd}(\text{Hflu})_2(\text{NO}_3)](\text{NO}_3)$ **1**, $[\text{Cd}(\text{H}_2\text{O})(\text{Hflu})_2(\text{Hmalo})](\text{NO}_3) \cdot 2(\text{H}_2\text{O})$ **2**, and $[\text{Cd}(\text{H}_2\text{O})(\text{Hflu})_2(\text{Hfum})](\text{NO}_3) \cdot 2(\text{H}_2\text{O})$ **3** ($\text{Hflu} = [2-(2,4\text{-difluorophenyl})-1,3\text{-bis}(1,2,4\text{-triazol-1-yl})\text{-propan-2-ol}]$, $\text{H}_2\text{fum} = \text{fumaric acid}$, $\text{H}_2\text{malo} = \text{malonate acid}$) are synthesized by a solution diffusion method and characterized by single crystal X-ray diffraction methods, elemental analyses, IR spectroscopy as well as thermal analyses. In compound **1**, Cd(II) cations are bridged by fluconazole ligands to form 2D Cd—Hflu layers, and these layers are further connected by C—H···F hydrogen bonds to form a complicated 3D structure with the topology of $(4\cdot6\cdot8)(4\cdot6^4\cdot8^4\cdot10)(6\cdot3)$. Compounds **2** and **3** are isostructural, and in them the Cd(II) cations are bridged by fluconazole ligands to form a 2D network, which is connected by C—H···O hydrogen bonds to form a complicated 3D (3,4)-connected framework with the topology of $(4\cdot8^2)(4\cdot8^5)$.

DOI: 10.15372/JSC20160119

К e y w o r d s: Cd(II) complexes, fluconazole, crystal structures, topology.

INTRODUCTION

During the past decades, metal organic coordination polymers have been extensively studied because of their attractive network structures as well as the potential applications as functional materials in the aspects of catalysis, host-guest chemistry, gas storage, separations, magnetic properties, optical properties and so on [1—5]. It has been well known that the building block choice is efficient in the construction of such coordination architectures through assemblies of the familiar metal ions with a variety of bridging ligands in which the structural and functional information is familiarized [6]. As compared to coordination polymers with rigid ligands limiting the structures of possible products, researches focusing on those with flexible ligands have currently been undergoing an unprecedented development for their flexible nature which could not only generate the aesthetic beauty of frameworks (such as helix, borromean ring, and torus ring, etc.) [7—9], but be also beneficial for the controllable assembly of functional materials such as hybrid magnets [10—12] and porous frameworks [13, 14]. Among the flexible bridging ligands, a variety of α,ω -dicarboxylic acids and flexible heterocyclic ligand such as various 1,2-bis(4-pyridyl)-ethane and 1,3-bis(4-pyridyl)-propane have been widely employed [15, 16]. Out of the flexible ligands, the utilization of organic drug [2-(2,4-difluorophenyl)-1,3-bis(1,2,4-triazol-1-yl)-propan-2-ol] (Hflu) molecules as building blocks in crystal engineering of coordination polymers remains largely unexplored [17]. Hflu displays rich coordination



Scheme 1

modes (Scheme 1) because the nitrogen atoms from two terminal triazole groups and the alkoxo atom can chelate the metal ions safely to generate stable structures. Three carbon atoms bridge the two triazole ligands and the flexible C—C chain of fluconazole can be rotated for a suitable position and angle to fit the size and geometrical configuration of anions in the self-assembly of metal complexes. Apart from these, weak interactions from Hflu (hydrogen bonding) are also significant to stabilize the structure and/or to form high dimensional structures [18—20].

EXPERIMENTAL

Materials. All chemicals of reagent grade were commercially available and used without further purification.

Physical methods. Powder X-ray diffraction measurements were carried out with a Bruker D8 Focus X-ray diffractometer using CuK_α radiation with a wavelength of 1.54012 \AA at a scan speed of $10^\circ/\text{min}$ to check the phase purity. Single crystal X-ray diffraction data were collected using a Rigaku R-Axis Rapid X-ray diffractometer. The C, N and H microanalyses were performed on a Perkin Elmer 2400II elemental analyzer. The FT-IR spectra were recorded from KBr pellets in the range

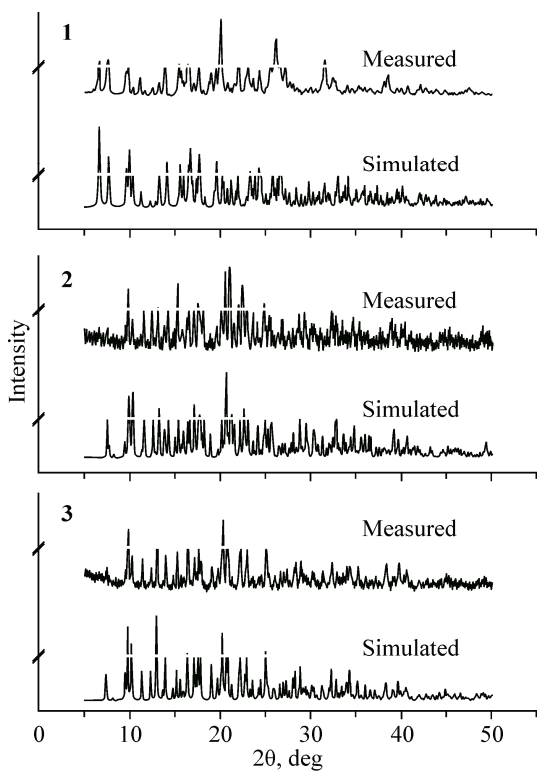


Fig. S1. Measured and simulated XRD patterns for 1–3

4000—400 cm^{-1} on a Shimadzu FTIR-8900 spectrometer. Thermogravimetric measurements were carried out from room temperature to 900 °C on preweighed samples in a nitrogen stream using a Seiko Exstar 6000 TG/DTA 6300 apparatus with a heating rate of 10 °C/min.

Synthesis of $[\text{Cd}(\text{Hflu})_2(\text{NO}_3)](\text{NO}_3)$ 1.

$\text{Cd}(\text{NO}_3)_2 \cdot 4\text{H}_2\text{O}$ (0.1540 g, 0.5 mmol) and Hflu (0.1530 g, 0.5 mmol) were separately dissolved in a mixed solvent of 5.0 ml H_2O and 5.0 ml CH_3OH . The dropwise addition of a Cd(II) solution to the stirred Hflu solution gave a clear solution. The resulting solution was kept at room temperature, and slow evaporation for two weeks afforded block colorless crystals (yield: ca. 36.7 % yield on the basis of the initial Hflu input). The powder XRD pattern of the compound matches well with that simulated based on the single crystal data. Anal. Calcd for $\text{C}_{26}\text{H}_{24}\text{CdF}_4\text{N}_{14}\text{O}_8$ (%): C 36.78, H 2.85, N 23.10. Found: C 36.94, H 2.98, N 23.23. IR data (cm^{-1} , KBr): 3123w, 3030w, 2932w, 2648w, 2538w, 1697vs, 1618s, 1522s, 1502m, 1420s, 1385vs, 1312s, 1277s, 1205s, 1176w, 1130s, 1094w, 1038m, 984w, 966s, 914w, 893w, 862w, 825w, 802w, 673w, 658w, 638w, 575w.

Synthesis of $[\text{Cd}(\text{H}_2\text{O})(\text{Hflu})_2(\text{Hmal})](\text{NO}_3) \cdot 2(\text{H}_2\text{O})$ 2. In a typical synthetic procedure, $\text{Cd}(\text{NO}_3)_2 \cdot 4\text{H}_2\text{O}$ (0.1540 g, 0.5 mmol), malonate acid (0.1180 g, 1.0 mmol), and Hflu (0.1530 g, 0.5 mmol) were separately dissolved in a mixed solvent of 5.0 ml H_2O and 5.0 ml CH_3OH . After the dropwise addition of the organic acid solution to the Cd(II) solution, the Hflu solution was added, giving a clear solution. The resulting solution was allowed to stand at room temperature. About 7 days later, colorless chip crystals (yield: ca. 39.8 % yield on the basis of the initial Hflu input) appeared in the solution and were isolated. The product was confirmed to be a pure phase by matching the experimental XRD pattern to the simulated one based on the single crystal data (Fig. S1). Anal. Calcd for $\text{C}_{29}\text{H}_{33}\text{CdN}_{13}\text{O}_{12}$ (%): C 36.89, H 3.52, N 19.29. Found (%): C 36.71, H 3.71, N 19.45. IR data (cm^{-1} , KBr): 3335m, 3115w, 1701m, 1618s, 1599w, 1522vs, 1501w, 1425m, 1383vs, 1278vs, 1211m, 1130vs, 1038m, 982s, 968s, 891m, 870s, 827w, 750w, 673s, 658s, 629m, 521s.

Synthesis of $[\text{Cd}(\text{H}_2\text{O})(\text{Hflu})_2(\text{Hfum})](\text{NO}_3) \cdot 2(\text{H}_2\text{O})$ 3. Complex 3 was synthesized similarly to 2 except that fumaric acid (0.1160 g, 1.0 mmol) was used instead of malonate acid. In 6 days the clear solution afforded platelet colorless crystals (yield: ca. 42.1 % yield on the basis of the initial Hflu input) and verified to be a pure phase by comparing the experimental XRD pattern with the simulated one based on the single crystal data. Anal. Calcd for $\text{C}_{30}\text{H}_{31}\text{CdF}_4\text{N}_{12}\text{O}_{12}$ (%): C 37.77, H 3.28, N 17.62. Found (%): C 37.92, H 3.47, N 17.43. IR data (cm^{-1} , KBr): 3309m, 3115m, 3057w, 1618s, 1522vs, 1501s, 1423w, 1385vs, 1279vs, 1213s, 1130s, 1094w, 1038w, 982s, 964s, 893m, 872m, 827w, 793w, 673s, 658s, 575w, 515m.

X-ray crystallography. Suitable single crystals were selected under a polarizing microscope and fixed with epoxy cement on respective fine glass fibres which were then mounted on a Rigaku R-Axis Rapid diffractometer with graphite-monochromated MoK_α radiation ($\lambda = 0.71073 \text{ \AA}$) for cell determination and subsequent data collection. The reflection intensities in the suitable θ ranges were collected at 293 K using the ω scan technique. The selected single crystals exhibited no detectable decay during the data collection. The data were corrected for Lp and absorption effects. The direct method employing the SHELXS-97 program [21] gave the initial positions for part of non-hydrogen atoms, and the

Table 1

Summary of the crystal data collection, structure solution and refinement details for **1**—**3** ($T = 293(2)$ K)

Compounds	1	2	3
Empirical formula	C ₂₆ H ₂₄ CdF ₄ N ₁₄ O ₈	C ₂₉ H ₃₃ CdN ₁₃ O ₁₂	C ₃₀ H ₃₁ CdF ₄ N ₁₂ O ₁₂
Formula weight	849.00	944.09	954.09
Crystal system	Triclinic	Monoclinic	Monoclinic
Description	Colorless, block	Colorless, platelet	Colorless, chip
Crystal size, mm	0.40×0.38×0.31	0.48×0.39×0.13	0.46×0.35×0.33
Space group	$P\bar{1}$	$P2_1/c$	$P2_1/c$
a , Å	10.608(2)	12.055(2)	12.146(2)
b , Å	11.846(2)	14.096(3)	14.388(3)
c , Å	13.718(3)	22.605(7)	22.698(7)
α , deg.	88.92(3)	90	90
β , deg.	76.14 (3)	107.30(3)	105.65(3)
γ , deg.	77.45(3)	90	90
Volume, Å ³	1632.7(6)	3667.4(16)	3819.6(17)
Z	2	4	4
D_c , g/cm ³	1.727	1.710	1.659
$F(000)$	852	1912	1928
μ , mm ⁻¹	0.76	0.70	0.67
θ range, deg.	3.05—27.48	3.07—27.48	3.13—27.46
Reflections collected	16045	34115	36386
Unique reflections(R_{int})	7487 ($R_{int} = 0.057$)	8411 ($R_{int} = 0.0718$)	8749 ($R_{int} = 0.046$)
Data, restraints, parameters	6004, 1, 486	7553, 3, 540	7397, 0, 553
Goodness of fit on F^2	1.087	1.073	0.801
R_1 , wR_2 [$I \geq 2\sigma(I)$] ^a	0.0501, 0.1190	0.0335, 0.0900	0.0309, 0.0893
R_1 , wR_2 (all data) ^a	0.0651, 0.1387	0.0395, 0.0936	0.0396, 0.1006
A , B values in w ^b	0.0361, 6.0018	0.0447, 3.2496	0.0721, 5.6422
$\delta\rho_{\max}$, $\delta\rho_{\min}$, e/Å ³	1.618, -1.762	0.917, -0.837	0.614, -0.748

^a $R_1 = \sum(|F_0| - |F_c|) / \sum|F_0|$, $wR_2 = [\sum w(F_0^2 - F_c^2)^2 / \sum w(F_0^2)]^{1/2}$.^b $w = [\sigma^2(F_0^2) + (AP)^2 + BP]^{-1}$ with $P = (F_0^2 + 2F_c^2)/3$.

subsequent difference Fourier syntheses using the SHELXL-97 program [22] resulted in the initial positions for the other non-hydrogen atoms. The hydrogen atoms attached to the carbon atoms were geometrically generated, while the remaining hydrogen atoms were located from the successive difference Fourier syntheses. The full-matrix least-squares technique was applied for the refinement of positions and anisotropic displacement parameters of all the non-hydrogen atoms, and positions of the hydrogen atoms were refined using the riding mode by fixing the initial distances to the associated heavier atoms with the isotropic displacement parameters set to 1.2 times of the values for the associated atoms. Detailed information about the crystal data and structure determination is summarized in Table 1. Selected interatomic distances and bond angles are given in Tables 2—4.

RESULTS AND DISCUSSION

Description of the crystal structures. $[Cd(Hflu)_2(NO_3)](NO_3)$ **1**. The asymmetric unit of **1** consists of one Cd²⁺ ion, two Hflu molecules, one coordinated NO₃⁻ anion, and one free NO₃⁻ anion. As

Table 2

Selected interatomic distances (\AA) and bond angles (deg.) for 1

Cd1—O3	2.433(3)	O3—Cd1—O5 ^{#2}	92.09(18)	N1—Cd1—N7	90.82(14)
Cd1—N4 ^{#1}	2.265(4)	O3—Cd1—N7	84.62(13)	N4 ^{#1} —Cd1—N10 ^{#3}	94.91(13)
Cd1—O5 ^{#2}	2.308(5)	O5 ^{#2} —Cd1—N4 ^{#1}	104.32(17)	O3—Cd1—N4 ^{#1}	87.22(13)
Cd1—N7	2.283(4)	N1—Cd1—N4 ^{#1}	86.53(13)	O5 ^{#2} —Cd1—N1	167.95(15)
Cd1—N1	2.353(4)	N4 ^{#1} —Cd1—N7	171.67(13)	O5 ^{#2} —Cd1—N10 ^{#3}	92.91(18)
Cd1—N10 ^{#3}	2.327(4)	O3—Cd1—N1	83.09(13)	N1—Cd1—N10 ^{#3}	91.33(13)
		O3—Cd1—N10 ^{#3}	173.90(12)	N7—Cd1—N10 ^{#3}	93.05(13)
O5 ^{#2} —Cd1—N7					77.70(17)
D—H···A	D—H	H···A	D···A	\angle DHA	
Hydrogen bonding contacts					
O1—H11···O8	0.78	1.99	2.72	155	C25—H25A···F2 ^{#4}
O2—H21···O8	0.89	1.89	2.77	164	0.93
Hydrogen bonding contacts					
					2.55
					3.04
					113

Symmetry transformations used to generate equivalent atoms: ^{#1} $x+1, y, z$; ^{#2} $-x+3, -y, -z+1$; ^{#3} $-x+2, -y+1, -z+1$; ^{#4} $-x, 1-y, -z$.

Table 3

Selected interatomic distances (\AA) and bond angles (deg) for 2

Cd1—O3	2.270(2)	O3—Cd1—O7	88.36(7)	N1—Cd1—N7	104.97(7)
Cd1—N4 ^{#2}	2.378(2)	O3—Cd1—N7	104.41(7)	N4 ^{#2} —Cd1—N10 ^{#1}	85.27(6)
Cd1—O7	2.325(1)	O7—Cd1—N4 ^{#2}	81.21(6)	O3—Cd1—N4 ^{#2}	84.77(7)
Cd1—N7	2.294(2)	N1—Cd1—N4 ^{#2}	90.66(7)	O7—Cd1—N1	171.04(5)
Cd1—N1	2.316(2)	N4 ^{#2} —Cd1—N7	162.07(7)	O7—Cd1—N10 ^{#1}	90.93(6)
Cd1—N10 ^{#1}	2.371(2)	O3—Cd1—N1	87.15(7)	N1—Cd1—N10 ^{#1}	92.14(7)
		O3—Cd1—N10 ^{#1}	170.01(6)	N7—Cd1—N10 ^{#1}	85.41(6)
O7—Cd1—N7					83.66(6)
D—H···A	D—H	H···A	D···A	\angle DHA	
Hydrogen bonding contacts					
O1—H51···O10 ^{#1}	0.75	2.02	2.75	164	O11—H111···O5 ^{#4}
O2—H11···O8	0.69	2.53	3.19	162	O11—H112···O9
O6—H61···O4	0.83	1.68	248	161	O12—H121···N8 ^{#5}
O7—H71···O5 ^{#3}	0.85	1.94	2.79	180	O12—H122···O11 ^{#5}
O7—H72···O8	0.84	2.00	2.84	180	C21—H21B···O6 ^{#6}
Hydrogen bonding contacts					
					0.83
					2.36
					3.15
					158
					0.98
					2.08
					2.96
					148
					0.89
					2.29
					3.17
					170
					0.90
					2.04
					2.90
					160
					0.97
					2.42
					3.26
					145

Symmetry transformations used to generate equivalent atoms: ^{#1} $x, -y-3/2, z-1/2$; ^{#2} $-x, -y-2, -z-2$; ^{#3} $-x, y+1/2, -z-3/2$; ^{#4} $x, y+1, z$; ^{#5} $-x-1, y-1/2, -z-3/2$; ^{#6} $-x-1, 1/2+y, -3/2-z$.

illustrated in Fig. 1, the Cd(II) ion is six-coordinated by four triazolyl—N atoms from four Hflu ligands, one oxygen atom from the monodentate NO_3^- anion, and an aqua ligand to form a slightly distorted octahedral sphere. The Cd—N bond distances range from 2.265(4) \AA to 2.353(4) \AA , while Cd—O bond lengths fall in the range of 2.308(5)—2.433(3) \AA (Table 4). The cisoid bond angles around the Cd(II) ion fall in the range of 77.7—104.3°, and the transoid ones are 168.0—173.9°, ex-

Table 4

Selected interatomic distances (\AA) and bond angles (deg.) for **3**

Cd1—O3	2.308(2)	O3—Cd1—O7	93.39(8)	N1—Cd1—N7	92.67(8)				
Cd1—N4 ^{#1}	2.291(2)	O3—Cd1—N7	86.66(9)	N4i—Cd1—N10 ^{#2}	166.50(8)				
Cd1—O7	2.359(2)	O7—Cd1—N4 ^{#1}	80.84(7)	O3—Cd1—N4 ^{#1}	87.41(8)				
Cd1—N7	2.323(2)	N1—Cd1—N4 ^{#1}	88.37(7)	O7—Cd1—N1	87.47(8)				
Cd1—N1	2.347(2)	N4 ^{#1} —Cd1—N7	101.69(8)	O7—Cd1—N10 ^{#2}	85.72(7)				
Cd1—N10 ^{#2}	2.355(2)	O3—Cd1—N1	175.50(7)	N1—Cd1—N10 ^{#2}	89.81(8)				
		O3—Cd1—N10 ^{#2}	94.67(8)	N7—Cd1—N10 ^{#2}	91.75(8)				
		O7—Cd1—N7	177.47(7)						
D—H···A	D—H	H···A	D···A	\angle DHA	D—H···A	D—H	H···A	D···A	\angle DHA
Hydrogen bonding contacts					Hydrogen bonding contacts				
O1—H11···O10 ^{#3}	0.69	2.34	3.03	173	O11—H112···O12 ^{#6}	0.85	2.12	2.97	180
O2—H21···O8 ^{#3}	0.83	1.98	2.78	163	O12—H121···O5	0.84	2.02	2.86	180
O6—H61···O4 ^{#4}	1.14	1.31	2.45	172	O12—H122···O9 ^{#7}	0.85	2.23	3.08	180
O11—H111···N5 ^{#5}	0.85	2.26	3.11	180	C11—H11B···O5 ^{#8}	0.97	2.29	3.13	145

Symmetry transformations used to generate equivalent atoms: ^{#1} $x, -y-3/2, z-1/2$; ^{#2} $-x, -y-1, -z$; ^{#3} $-x+1, -y-1, -z$; ^{#4} $-x, y+1/2, -z-1/2$; ^{#5} $-x+1, -y-1, -z$; ^{#6} $-x+1, y-1/2, -z-1/2$; ^{#7} $-x+1, y+1/2, -z-1/2$; ^{#8} $1-x, 1-y, -z$.

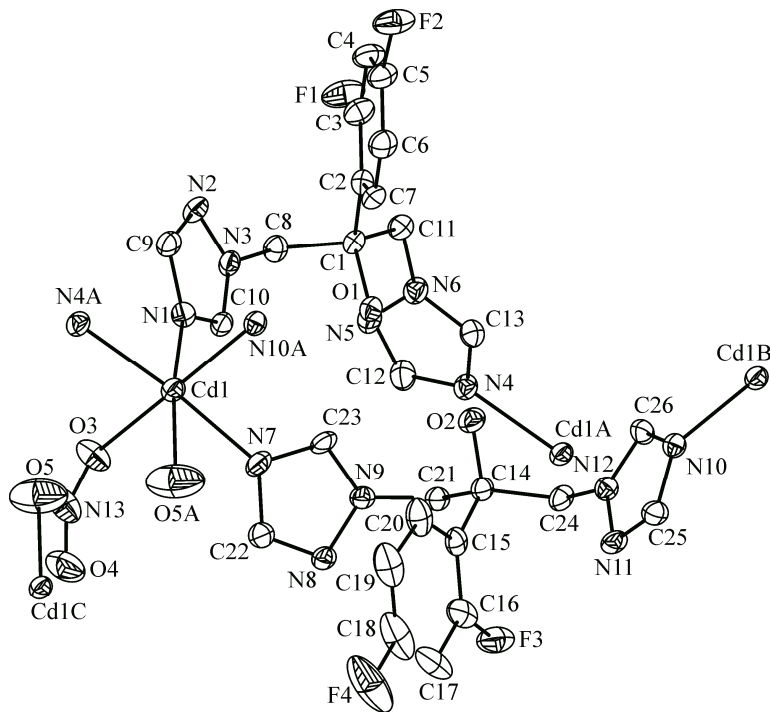


Fig. 1. ORTEP view of the molecule of $[\text{Cd}(\text{Hflu})_2(\text{NO}_3)](\text{NO}_3)$ complex **1** with displacement ellipsoids (45 % probability) and atomic labeling

hibiting a significant departure from the corresponding value for a regular square pyramid (90° and 180°). In **1**, there are two kinds of Hflu ligands, the $\eta^2\mu_2$ coordination mode (type *c* and *d* in Scheme 1), namely Hflu(*c*) and Hflu(*d*) which contain N1 and N7 atoms, respectively. They have dif-

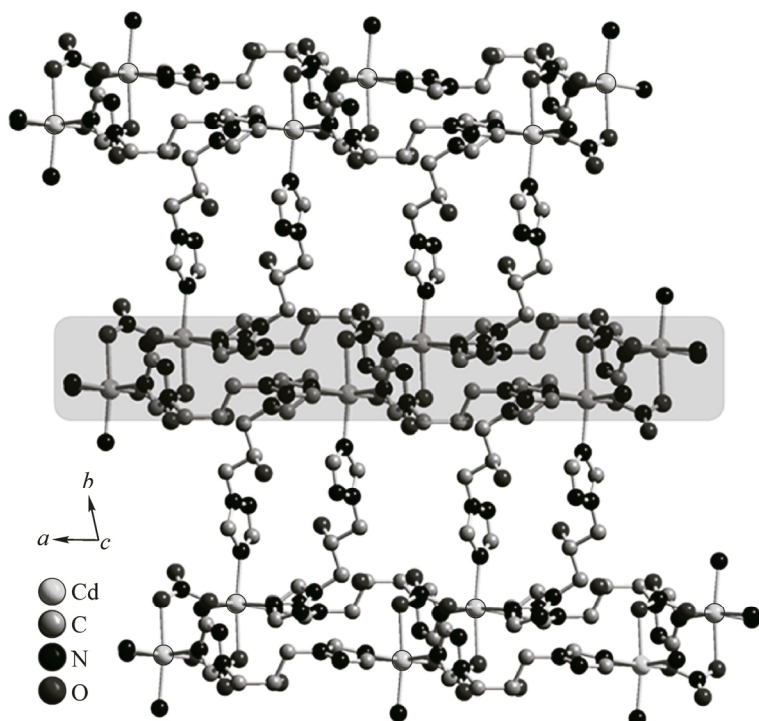


Fig. 2. View of the infinite 2D structure of **1**

ferent configurations, *trans*- and *cis*-conformations. In Hflu(c), the dihedral angle between two triazole rings is 83.0°, and the dihedral angle between the triazole ring and the phenyl ring is 54.8° or 43.3°. In Hflu(d), the corresponding dihedral angles are 80.0° and 39.6° or 64.9°, respectively. The dihedral angle between the two phenyl rings from two different Hflu ligands is 41.7°. These ligands twist to meet the requirement of steric exclusion. The torsion angles are 79.7° for N6—C11—C1—C8 and -179.4° for C11—C1—C8—N3 in Hflu(c), and -175.2° for N9—C21—C14—C24 and -179.1° for C21—C14—C24—N12 in Hflu(d).

The Hflu(c) ligand bridges two Cd(II) atoms to form a single 1D chain, and two Cd(II) atoms from the parallel single chain are bridged by two NO_3^- ions to form the ribbons with the Cd···Cd distance of 4.827(3) Å. Due to this type of interactions, the double 1D chains propagate infinitely in the [100] direction and *via* the other two Hflu(d) ligands are bridging to two Cd(II) atoms to form a 20-membered macrocyclic fragment with the Cd···Cd distance of 11.361(3) Å, assembled into two-dimension layers parallel to (001) (Fig. 2). Simultaneously, the Hflu(d) ligand C25 donates the hydrogen atom to another Hflu(c) molecule F2 to form an interlayer hydrogen bond with $d(\text{C}25\text{—H}\cdots\text{F}2^{\#1}) = 3.04$ Å, $\angle(\text{C}25\text{—H}\cdots\text{F}2^{\#1}) = 113^\circ$. Due to these types of interactions, the molecules are assembled into a 3D framework extending along the [001] direction (symmetry codes: #1 $-x, 1-y, -z$). When C—H···F hydrogen bonding interactions in **1** can be taken into topological considerations, the Hflu molecule, due to the engagement in bridging to two Cd atoms and in hydrogen bonds to another Hflu neighbor, is in turn three-connected with a vertex symbol of (4·6·8), and the NO_3^- ligands are treated as a two-connected node. The Cd atoms are linked to four Hflu ligands *via* the covalent bond as well as the hydrogen bonding and one Cd atom with a vertex symbol of (4·6⁴·8⁴·10). As a result, the 3D supramolecular architecture of **1** could be topologically described as a 3D (3,5)-connected network with the Schläfli symbol (4·6·8)(4·6⁴·8⁴·10)(6·3) as illustrated in Fig. 3. To the best of our knowledge, complex **1** represents an unprecedented example of a novel network topology that has never yet been reported by the others.

[Cd(H₂O)(Hflu)₂(Hmalo)](NO₃)·2(H₂O) **2** and **[Cd(H₂O)(Hflu)₂(Hfum)](NO₃)·2(H₂O)** **3**. The ORTEP drawings of complexes **2** and **3**, which possess a two-dimensional network with the covalent

Fig. 3. Topological representation of the 3D supramolecular architecture in **1**

bonding is given in Fig. 4. Both isostructural compounds **2** and **3** crystallize in the monoclinic space group $P2_1/c$. Within the asymmetric unit of **2** there are one Cd^{2+} ion, two Hflu molecules (namely Hflu(d)1 and Hflu(d)2, which contain the N1 and N7 atoms, respectively), one Hmalo⁻ anion (one Hfum⁻ anion for **3**), one NO_3^- anion, one coordinated water molecule, and two free water molecules. The six-coordinated cadmium atoms adopt a slightly distorted octahedral coordination environment by coordinating to four triazolyl nitrogen atoms from four different Hflu ligands, one carboxylic oxygen atom from the Hfum ligand, and an aqua ligand with $\text{Cd}-\text{N(O)}$ distances of 2.270(2)–2.378(2) Å for **2** (2.291(2)–2.359(2) Å for **3**). The $\text{Cd}-\text{O}$ and $\text{Cd}-\text{N}$ distances are quite similar to normal $\text{Cd}-\text{O}$ and $\text{Cd}-\text{N}$ [23, 24]. The cisoid and transition angles around Cd atoms fall in the ranges of 81.2–105.0° and 162.0–171.0° for **2** (for **3**: 80.8–101.7° and 166.5–177.5°) (Tables 3 and 4), respectively, exhibiting a significant departure from 90° to 180°. The corresponding dihedral angle of the two triazole planes in Hflu are 63.3°, 70.2° for **2** (62.2°, 67.9° for **3**). The Hflu(d)2 ligand adopts $\eta^2\mu_2$ coordination mode (type *d* in Scheme 1) to two Cd(II) ions in the *cis* conformation with the $\text{Cd}\cdots\text{Cd}$ separation of 11.566(4) Å for **2** (11.571(4) Å for **3**), being slightly shorter than that in **3**. As a result of this type of interactions, the 1D chains propagate infinitely in the [001] direction and *via* the other two Hflu(d)1 ligands are bridging to two crystallographically equivalent

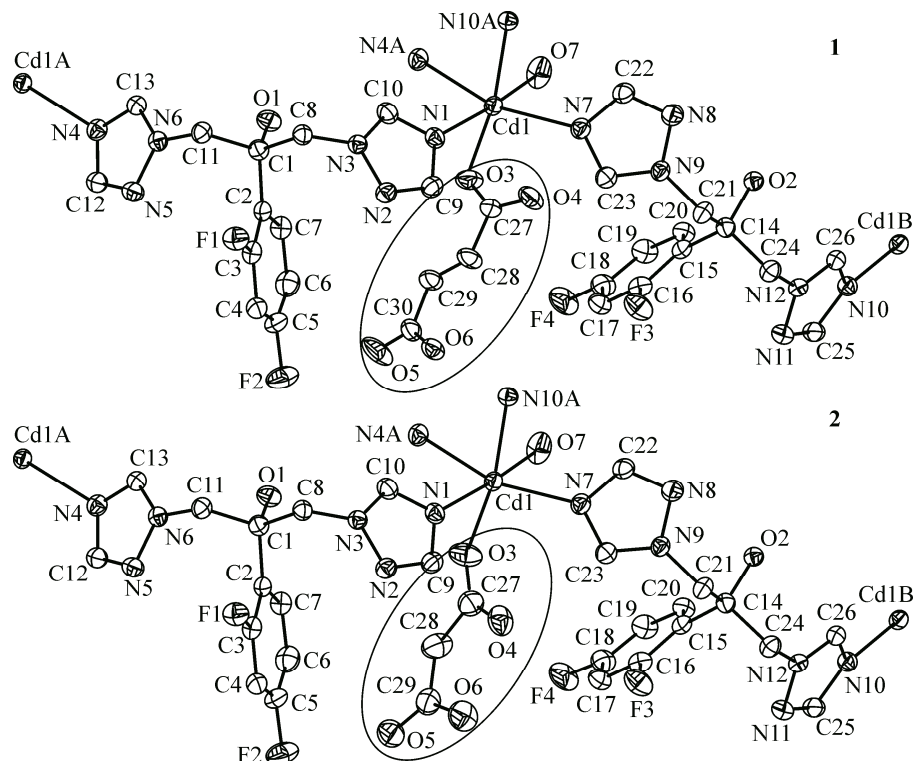
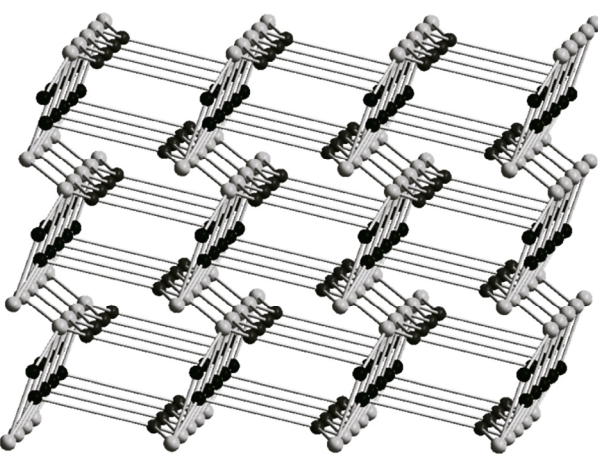


Fig. 4. ORTEP view of the molecules of $[\text{Cd}(\text{H}_2\text{O})(\text{Hflu})_2(\text{Hmalo})](\text{NO}_3)\cdot 2(\text{H}_2\text{O})$ **2** and $[\text{Cd}(\text{H}_2\text{O})(\text{Hflu})_2(\text{Hfum})](\text{NO}_3)\cdot 2(\text{H}_2\text{O})$ **3** complexes with displacement ellipsoids (45 % probability) and atomic labeling

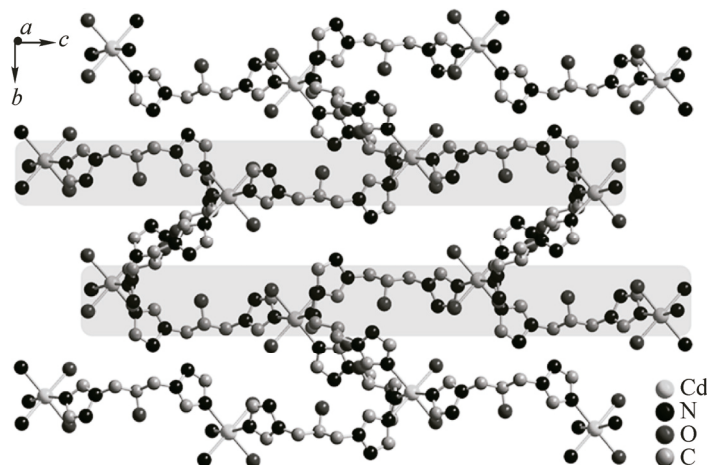


Fig. 5. View of the infinite 2D structures of **2** and **3**

Cd(II) atoms to generate a 20-membered macrocyclic fragment with the Cd···Cd distance of 11.409(2) Å for **2** (11.400(3) Å for **3**), assembled into two-dimension layers parallel to (100) (Fig. 5). The resulting 2D layers are also stabilized by O—H···O and O—H···N bonding interactions. Along the crystallographic *a* axis, the 2D layers are stacked, and interlayer hydrogen bonds from Hflu (C21 for **2**, C11 for **3**) ligands to oxygen atoms of the uncoordinating carboxylate groups of the malonate anion for **2** (fumaric anion for **3**) with $d(\text{C21}—\text{H}\cdots\text{O6}^{\#1}) = 3.26$ Å, $\angle(\text{C21}—\text{H}\cdots\text{O6}^{\#1}) = 145^\circ$ for **2** ($d(\text{C11}—\text{H}\cdots\text{O5}^{\#2}) = 3.13$ Å, $\angle(\text{C11}—\text{H}\cdots\text{O5}^{\#2}) = 145^\circ$ for **3**) are responsible for the stabilization of a 3D framework (symmetry codes: #1 $-1-x, 1/2+y, -3/2-z$; #2 $1-x, 1-y, -z$). Topologically, if the hydrogen bonding interactions (C11—H···O5 bonding interactions) are taken into consideration, the Hflu molecules are treated as a three-connected T-shaped node, and the Cd atoms as a 4-connecting node, which link three neighboring Hflu molecules via the covalent bond as well as the hydrogen bonding and bridge one Cd atom. The connectivity of **2** and **3** can be simplified as a (3,4)-connected 3D network and the overall Schläfli symbol can be described as a $(4\cdot8^2)(4\cdot8^5)$ topology as shown in Fig. 6.

Infrared spectra. IR spectra of **1**—**3** (Fig. S2) show features attributable to each component of the complexes and are compatible with the structures. For **1**, the absorption band appeared around ca. 3123 cm⁻¹ with weak intensity indicates the O—H stretching of the hydroxyl group from fluconazole. The bands centered at 1522, 1502, 1420 cm⁻¹ attributed to the C=N and C=C vibrations, and the weak absorption peaks observed at 3030 and 825, 802 cm⁻¹ can be ascribed to the $\nu_{\text{C}-\text{H}}$ stretching vibrations and out-of-plane C—H vibrations, respectively. The absorption bands centered at 3335, 3115 cm⁻¹ for **2** and 3309, 3115 cm⁻¹ for **3** are obviously due to the O—H stretching vibrations of the lattice water molecules, coordinated water molecule and the Hflu ligand. According to the spectra of Hflu, the absorption peaks at 1599, 1522, 1383 cm⁻¹ for **2** and 1522, 1501, 1385 cm⁻¹ for **3** are assigned to the C=N and C=C vibrations of the phenyl and triazole rings. The $\nu_{\text{C}-\text{H}}$ stretching vibrations result in a

weak absorption at 3115 cm⁻¹ for **2** and 3057 cm⁻¹ for **3**, and the out-of-plane C—H vibrations lead to absorptions at 870, 673, 658 cm⁻¹ for **2** and 872, 673, 658 cm⁻¹ for **3**, respectively. The strong absorption bands centered at 1618 cm⁻¹ for **2** and **3**, respectively, could be ascribed to the asymmetric stretching vibration

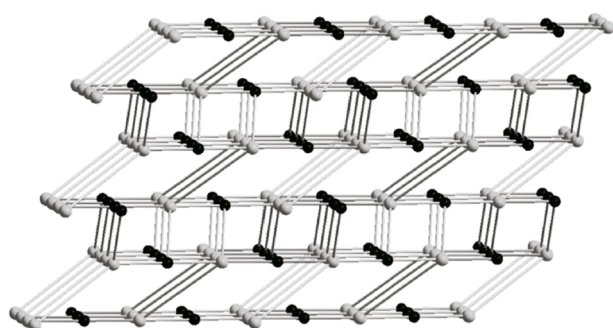
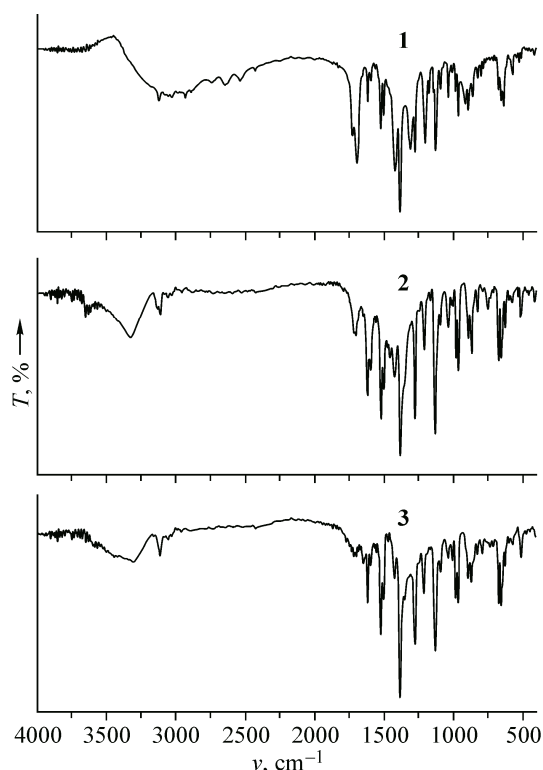
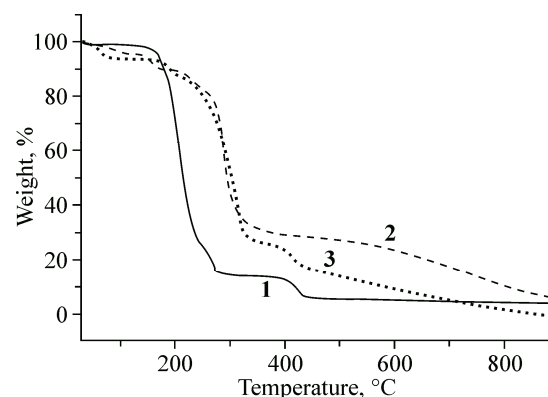


Fig. 6. Topological representation of the 3D supramolecular architecture in **2** and **3**

Fig. S2. Infrared spectra of **1—3**Fig. S3. Thermogravimetric curves for **1—3**

of $-\text{COO}$ groups, while the symmetric stretching vibration of $-\text{COO}$ groups results in absorptions at 1383 cm^{-1} for **2** and 1385 cm^{-1} for **3**. The differences ($\nu_{\text{as}} - \nu_s$) are 235 cm^{-1} for **2**, 233 cm^{-1} for **3**, consistent with the monodentate coordination mode for **2** and **3** according to correlation of the $\Delta\nu_{\text{as-s}}$ magnitude with the coordination modes of carboxylate groups [25].

Thermal analysis. Thermogravimetric measurements were performed from room temperature to $900\text{ }^\circ\text{C}$ on preweighed samples of **1—3** in a nitrogen stream with a heating rate of $10\text{ }^\circ\text{C}/\text{min}$ (Fig. S3). Thermal analyses show **1** to be stable below $120\text{ }^\circ\text{C}$. The observed rapid weight loss at the first step in the range 120 — $320\text{ }^\circ\text{C}$ reaches 86.12 \% , which is close to the calculated value (86.76 \%) for the gradual decomposition and collapse of the organic skeleton. Upon further heating, decomposition continues in continuous steps to give a final black solid until $900\text{ }^\circ\text{C}$. For complex **2**, the first observed weight loss in the range of 30 — $140\text{ }^\circ\text{C}$ (5.18 \%) is in agreement with the calculated value of 5.72 \% for the loss of one coordinated water and two lattice water molecules per formula unit. Then the weight loss above $140\text{ }^\circ\text{C}$ can be assigned to the release of organic components, and the residue decomposed with the tendency to form a black solid. Complex **3** loses 5.66 \% of the total weight in the temperature range of 30 — $110\text{ }^\circ\text{C}$, corresponding to the loss of one coordinated water and two lattice water molecules per formula (exp: 5.65 \%), and then upon further heating, the resulting intermediate undergoes the gradual decomposition and collapse of the organic skeleton. The final black solid residual was collected at $900\text{ }^\circ\text{C}$.

CONCLUSIONS

The fluconazole ligand shows good flexible nature to bridge two Cd(II) ions through two triazolyl nitrogen atoms with *trans-/cis*-conformations to fulfil the geometric requirement of Cd(II) ions and three compounds, $[\text{Cd}(\text{Hflu})_2(\text{NO}_3)](\text{NO}_3)$ **1**, $[\text{Cd}(\text{H}_2\text{O})(\text{Hflu})_2(\text{Hmalo})](\text{NO}_3) \cdot 2(\text{H}_2\text{O})$ **2**, and $[\text{Cd}(\text{H}_2\text{O})(\text{Hflu})_2(\text{Hfum})](\text{NO}_3) \cdot 2(\text{H}_2\text{O})$ **3** have been synthesized by a solution diffusion method under similar conditions except different anions. The crystal structure of complex **1** represents a (3,5)-connected 3D supramolecular architecture network with the Schläfli symbol $(4\cdot6\cdot8)(4\cdot6^4\cdot8^4\cdot10)(6\cdot3)$. Compounds **2** and **3** exhibit similar 2D structures connected by C—H \cdots O hydrogen bonds to form a complicated 3D (3,4)-connected framework with the topology of $(4\cdot8^2)(4\cdot8^5)$.

This project was sponsored by K.C. Wong Magna Fund in Ningbo University and supported by the Scientific Research Fund of Zhejiang Provincial Education Department.

Supplementary material. Details of the data collection and refinement, fractional atomic coordinates, anisotropic displacement parameters, and full list of bond lengths and angles are in CIF format. Crystallographic data for the compound have been deposited with the Cambridge Crystallographic Data Center, CCDC 1027700 (1), 1027702 (2) and 1027701 (3). Copies of this information may be obtain free of charge from the Director, CCDC, 12 Union Road, Cambridge CB2 1EZ, United Kingdom (Fax: (44)1223-336-033. E-mail: deposit@ccdc.cam.ac.uk. Website: <http://www.ccdc.cam.ac.uk>).

REFERENCES

1. Corma A., Rey F., Rius J., Sabater M.J., Valencia S. // *Nature*. – 2004. – **431**. – P. 287 – 290.
2. Schmitt W., Baissa E., Mandel A., Anson C.E., Powell A.K. // *Angew. Chem., Int. Ed.* – 2001. – **40**, N 19. – P. 3577 – 3581.
3. Sozzani P., Bracco S., Comotti A., Ferretti L., Simonutti R. // *Angew. Chem., Int. Ed.* – 2005. – **44**, N 12. – P. 1816 – 1820.
4. Campidelli S., Brandmüller T., Hirsch A., Saez I.M., Goodby J.W., Deschenaux R. // *Chem. Commun.* – 2006. – P. 4282 – 4284.
5. Petitjean A., Puntoniero F., Campagna S., Juris A., Lehn J.M. // *Eur. J. Inorg. Chem.* – 2006. – P. 3878 – 3892.
6. Janiak C. // *Dalton Trans.* – 2003. – P. 2781 – 2804.
7. Xiong R.G., Zuo J.L., You X.Z., Abrahams B.F., Bai Z.P., Che C.M., Fun H.K. // *Chem. Commun.* – 2000. – P. 2061 – 2062.
8. Wang X.L., Qin C., Wang E.B., Xu L., Su Z.M., Hu C.W. // *Angew. Chem.* – 2004. – **116**. – P. 5146 – 5150.
9. Lloyd G.O., Atwood J.L., Barbour L.J. // *Chem. Commun.* – 2005. – P. 1845 – 1847.
10. Carballo R., Covelo B., Fallah M.S.E., Ribas J., Vazquez-Lopez E.M. // *Cryst. Growth Des.* – 2007. – **7**. – P. 1069 – 1077.
11. Li R.Y., Wang X.Y., Liu T., Xu H.B., Zhao F., Wang Z.M., Gao S. // *Inorg. Chem.* – 2008. – **47**. – P. 8134 – 8142.
12. Couceiro U.G., Castillo O., Luque A., Teran J.P.G., Beobide G., Roman P. // *Cryst. Growth Des.* – 2006. – **6**. – P. 1839 – 1847.
13. Maji T.K., Matsuda R., Kitagawa S. // *Nat. Mater.* – 2007 – **6**. – P. 142 – 148.
14. Zhang J.P., Chen X.M. // *J. Am. Chem. Soc.* – 2008. – **130**. – P. 6010 – 6017.
15. Mukherjee P.S., Konar S., Zangrando E., Mallah T., Ribas J., Chaudhuri N.R. // *Inorg. Chem.* – 2003. – **42**. – P. 2695 – 2703.
16. Suen M.C., Chan Z.K., Chen J.D., Wang J.C., Hung C.H. // *Polyhedron*. – 2006. – **25**, N 11. – P. 2325 – 2332.
17. Su L.J., Zang H.Y., Liu H.S., Wang L.M., Li W.H., Su Z.M. // *Inorg. Chem. Commun.* – 2010. – **13**. – P. 981.
18. Roesky H.W., Andruh M. // *Coord. Chem. Rev.* – 2003. – **236**. – P. 91.
19. Kitagawa S., Uemura K. // *Chem. Soc. Rev.* – 2005. – **34**. – P. 109.
20. Keizer H.M., Sijbesma R.P. // *Chem. Soc. Rev.* – 2005. – **34**. – P. 226.
21. Sheldrick G.M., SHELXS-97, Program for Crystal Structure Solution. – Germany: University of Göttingen, 1997.
22. Sheldrick G.M., SHELXS-97, Program for Crystal Structure Refinement. – Germany: University of Göttingen, 1997.
23. Luan X.J., Cai X.H., Wang Y.Y., Li D.S., Wang C.J., Liu P., Hu H.M., Shi Q.Z., Peng S.M. // *Chem. Eur. J.* – 2006. – **12**. – P. 6281.
24. Wang R., Hong M., Luo J., Cao R., Weng J. // *Chem. Commun.* – 2003. – P. 1018.
25. Nakamoto K. // Infrared and Raman Spectra of Inorganic and Coordination Compounds. – 4th ed. – New York: Interscience-Wiley, 1986.